Journal of
Materials Chemistry B

Accepted Manuscript

This article can be cited before page numbers have been issued, to do this please use: H. Zhou, J. Peng, X. Qiu, Y. gao, L. Lu and W. Wang, *J. Mater. Chem. B*, 2017, DOI: 10.1039/C7TB01389B.

ROYAL SOCIETY OF CHEMISTRY

rsc.li/materials-b

ROYAL SOCIETY OF CHEMISTRY View Article Online
DOI: 10.1039/C7TB01389B

Journal of Materials Chemistry B

ARTICLE

β -Ni(OH)$_2$ nanosheet: an effective sensing platform for constructing nucleic acid-based optical sensor

Received 00th January 20xx,
Accepted 00th January 20xx

DOI: 10.1039/x0xx00000x

www.rsc.org/

Hui Zhou,[ab] Junbin Peng [b] Xinlan Qiu,[a] Yansha Gao,[a] Limin Lu,*[a] and Wenmin Wang[a]

In this study, beta nickel hydroxide (β-Ni(OH)$_2$) nanosheet, one of the transition metal oxyhydroxides with two dimensional (2D) structures, was explored as a new fluorescent biosensor platform and applied in constructing optical sensor for bioanalysis. It was found that β-Ni(OH)$_2$ nanosheet displayed a high fluorescence quenching ability and different affinity toward single- versus double-stranded DNA. Moreover, the absorption property of β-Ni(OH)$_2$ nanosheet can be well controlled by changing cations, solution pH and the length of DNA. In comparing with some reported 2D nanosheets platforms (e.g. graphene, metal chalcogenides), the absorbed DNA can also been desorbed by degrading the β-Ni(OH)$_2$ nanosheet, which is a simple but effective DNA desorption method. Based on these findings, a sensitive and selective optical miRNA sensor with a detection limit of 1 pM was demonstrated by combining the fluorescence quenching ability of β-Ni(OH)$_2$ nanosheet and duplex-specific nuclease signal amplification. The presented sensor has been successfully used for miRNA analysis in samples containing cancer cells and shown great potential in multiplexed miRNAs analysis for clinical diagnostics.

Introduction

MicroRNA (miRNA), a type of single-strand noncoding RNAs (21–23 nucleotides), functions as regulatory factors in a wide variety of biological processes via repression of mRNA translation.[1] Recently, it has been found that miRNA mutations or mis-expression correlate with various human diseases, especially for cancers. The actual expression level of one or, more commonly, of several miRNAs can be considered as a useful diagnostic and prognostic marker for practical applications.[2] However, detection of miRNAs is challenging due to their unique characteristics, such as small size, low abundance, and highly homologous among family members. Thus, developing simple, sensitive, selective and multiplex detection method for miRNAs is of great significance.

Among various miRNA detection methods, fluorescence-based techniques have attracted intense attentions due to their high sensitivity, simplicity and stability. By far, the current methods are developed mainly based on sequence-biased amplification mechanism (*e.g.* RT-PCR)[3,4] and isothermal amplification (*e.g.* RCA, EXPAR.[5,6] These strategies have good sensitivity for miRNAs, but suffering low selectivity, complicated design or time-consuming procedures. Numerous efforts have been put to optimize the performance of these sensors. Recently, Ye et al reported an elegant one-step fluorescence strategy for direct miRNA detection by using the duplex-specific nuclease (DSN) inducing miRNA recycling technique.[7] In which, Taqman DNA probe acted as a generalist to capture target miRNAs, cleave into short fragment and generate fluorescence signal continuously. Taking advantage of the particular properties of DSN, DSN signal amplification (DSNSA) assays is able to provide high sensitivity, selectivity and multiplex detection capability. However, in this system, to achieve the multiplex detection, Taqman probes are required to be labeled with specific quenchers to pair with dyes at the end. It follows Degliangeli et al optimized the quencher with gold nanoparticle to make DSNSA more suitable for multiplex detection.[2] In this system, gold nanoparticle was utilized as a public sensing platform to load and quench fluorophore-labeled probes. Jiang et al. described novel fluorescence assays combined WS_2 nanosheet sensing platform based fluorescence quenching with DSNSA for monitoring the miRNA.[8] Here, WS_2 nanosheets functioned as both dye-labeled single-stranded DNA (ssDNA) adsorbent and fluorescent dye quencher.

Beta nickel hydroxide (β-Ni(OH)$_2$) nanosheet is a transition metal oxyhydroxide combining two dimensional (2D) structures and the catalytic property of nickel-containing compounds. It has revealed great potential for lithium-ion batteries, photoelectrochemistry, supercapacitors, electroche-mical sensors and so on.[9-12] Despite of the significant progress in electrical applications, as far as we know, the use of β-Ni(OH)$_2$ nanosheet as a fluorimetric bioanalytical platform has not been explored. However, β-Ni(OH)$_2$ nanosheets possess similar characters as some reported 2D nanosheets, such as graphene oxide (GO), MoS_2, WS_2, MnO_2 and CoOOH.[8, 10,13-18] Most of them have been extensively used for biological applications owing to their unusual quantum properties and surface effects. Some of

[a] College of Science, Jiangxi Agricultural University, Nanchang 330045, P. R China. *E-mail: lulimin816@hotmail.com (L. M. Lu).
[b] College of Chemistry and Chemical Engineering, Gannan Normal University, Ganzhou 341000, P. R. China. *E-mail: huizhou314@163.com.
Electronic Supplementary Information (ESI) available: experimental details, supporting figures and tables. See DOI: 10.1039/x0xx00000x

View Article Online
DOI: 10.1039/C7TB01389B

them functioned as powerful quenchers not only for organic fluorescent dyes[19] but also for some fluorescent nanoparticles such as upconversion nanoparticles.[20, 21]

Herein, attempts of using β-Ni(OH)$_2$ nanosheet as a novel fluorimetric biosensing platform were carried out in this work. It is the first time finding that β-Ni(OH)$_2$ nanosheet can selectively adsorb fluorescent dye-labeled ssDNA and act as an efficient fluorescent dye quencher. The absorption can be modulated by changing the solution cations, pH and the length of ssDNA. Moreover, the adsorbed ssDNA can be effectively desorbed by degrading of β-Ni(OH)$_2$ nanosheet. Therefore, β-Ni(OH)$_2$ nanosheet was used as a fluorescent sensing platform and a DSNSA based optical sensor was developed for miRNA detection. This strategy combined the super fluorescence quenching ability of the β-Ni(OH)$_2$ nanosheets and the advantage of DSNSA. Additionally, the β-Ni(OH)$_2$ nanosheets can quench multiplexed dyes at the same time. Therefore, the assay is direct, simple, sensitive, selective and suitable for multiplexed miRNAs analysis.

Results and discussion

Characterization of β-Ni(OH)2 nanosheets

As can be seen from Fig. 1A, synthesized β-Ni(OH)$_2$ nanosheet has a nearly transparent flake-like shape with similar morphology reported by Jiang et al.[22] XRD patterns (Fig. 1B) clearly identify the well-crystallite Ni(OH)$_2$, where peaks located at 19.40°, 33.18°, 38.50°, 52.12° and 59.19° can be indexed as (001), (100), (101), (102), and (110) planes of hexagonal β-Ni(OH)$_2$ according to the standard JCPDS card (No. 14-0117). The intense and sharp diffraction peaks demonstrate that the product is well crystallized. Fig. 1C shows the FTIR spectrum of the β-Ni(OH)$_2$ nanosheet. The peaks located at 3430 cm-1 and 1631 cm^{-1} are attributed to vibrations of hydrogen-bonded O-H from the surface of β-Ni(OH)$_2$ nanosheet. The peak at 3645 cm^{-1} is assigned to non-hydrogen-bonded free O-H stretching vibration of the brucite-like sheet structure. The peak observed at 520 cm^{-1} is related to the deformation mode of free O-H. The peak at 1375 cm^{-1} is ascribed to the vibration of CO_3^{2-}, originating from the absorption of CO_2 in β-Ni(OH)$_2$ nanosheet.[23]

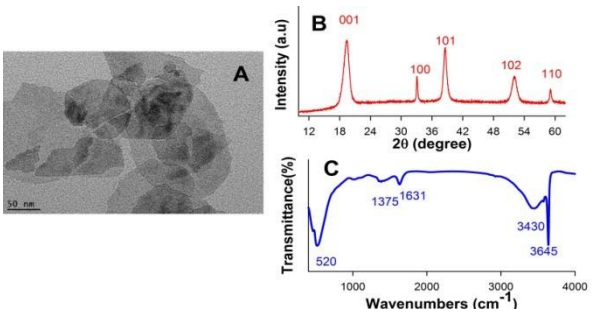

Fig. 1 TEM image (A), XRD pattern (B) and FTIR spectra (C) of β-Ni(OH)$_2$ nanosheets.

DNA adsorption

According to previous report, the isoelectric point of β-Ni(OH)$_2$ nanosheets is found to be 9.7.[24] At pH below 9.7, the surface of β-Ni(OH)$_2$ nanosheets is protonated. DNA is a polyanion containing aromatic and hydrophobic rings. Therefore, ssDNA is likely to be absorbed by β-Ni(OH)$_2$ nanosheets through electrostatic binding and the van der Waals force at a lower pH solution.[25,26] Based on that most transition-metal ions own intrinsic fluorescence quenching properties,[27] whether β-Ni(OH)$_2$ nanosheet could also act as an efficient fluorescent dye quencher? Following this consideration, we employed FAM-labeled 22-mer ssDNA (22-F) and corresponding dsDNA (22-F/DNA-141) to evaluate the adsorption property of β-Ni(OH)$_2$ nanosheets in homogeneous solution. Upon exciting ssDNA and dsDNA at 490 nm, both of them showed intense FAM emission at 518 nm (Fig. 2A). The addition of β-Ni(OH)$_2$ nanosheets brought the fluorescence of ssDNA to the baseline level, while the fluorescence of dsDNA was still high. The quenching efficiency of ssDNA and dsDNA were about 94% and 31%, respectively. This result confirms the speculation that β-Ni(OH)$_2$ nanosheets can effectively adsorb ssDNA, which indicates they can also act as a universal and efficient fluorescent quencher since the quenching efficiency is directly proportional to the amount of ssDNA adsorbed. In addition, according to the different quenching efficiency for ssDNA and dsDNA, the adsorb behavior of β-Ni(OH)$_2$ nanosheets is selective (Scheme 1). The lower adsorption for dsDNA may be relative with the fact that the aromatic and hydrophobic rings on dsDNA were hid inside the helical structure and there were no sites available for binding.[26] All the results are similar as the reported two-dimensional (2D) nanomaterials (e.g. graphene oxide, WS_2, MnO_2).[25,28,29] β-Ni(OH)$_2$ nanosheets possess two unique properties: selective absorption of DNA and effective quencher for dye-labeled ssDNA, which are the key points for 2D nanomaterials used as sensing platform in making DNA-based optical sensor.[26]

Another key point for 2D nanomaterials in making DNA-based optical sensor is the different affinity toward short ssDNA with different lengths.[8,18] We further test the absorbing and quenching efficiency of β-Ni(OH)$_2$ nanosheets for different ssDNAs. As shown in Fig. 2B, five FAM-labeled ssDNAs containing DNA lengths of 5-, 9-, 13-, 17- and 22-mer, respectively were exployed as templates and their absorption efficiency were tested in the same experiment condition. It is

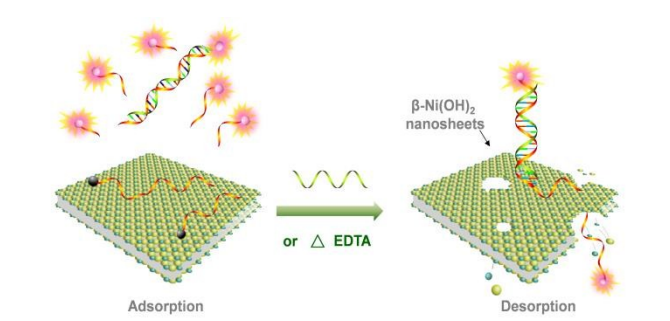

Scheme 1. Scheme for dye labeled DNA adsorbing and desorbing on nanosheets.

View Article Online
DOI: 10.1039/C7TB01389B

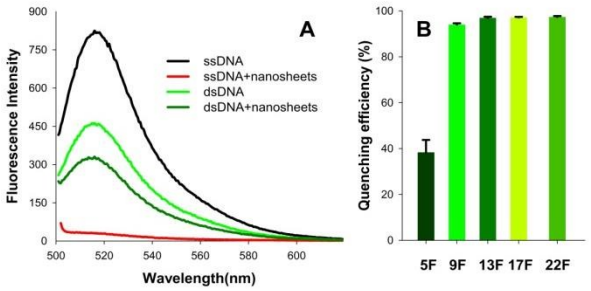

Fig. 2 A) Fluorescence spectra of ssDNA (22-F) and dsDNA (22-F/DNA-141) probes in the present and absence of 5 μL β-Ni(OH)$_2$ nanosheets (480 μg/mL); **B)** Fluorescence quenching efficiency (F_0-F/F_0) of 6 μL β-Ni(OH)$_2$ nanosheets for FAM-labeled ssDNA with different lengths. The concentrations of DNA were fixed at 50 nM in 20 mM Tris-HCl (pH 8.0) containing 100 mM KCl and 1 mM $MgCl_2$. The ssDNA of 5-F, 9-F, 13-F, 17-F, and 22-F denote the probes given in Table S1.

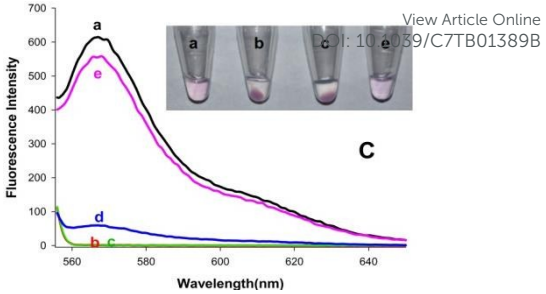

Fig. 3 Fluorescence spectra analysis of the supernatant of different samples: **(a)** 22-C; **(b)** 22-C + β-Ni(OH)$_2$ nanosheets; (c) 22-C + β-Ni(OH)$_2$ nanosheets + 95 °C heat treatment; (d) 22-C + β-Ni(OH)$_2$ nanosheets + EDTA; (e) 22-C + β-Ni(OH)$_2$ nanosheets +EDTA + 95 °C heat treatment. Each sample (25 μL) contained a final buffer concentration of 25 mM, 100 mM KCl, 1 mM $MgCl_2$, 0.96 mg/mL β-Ni(OH)$_2$ nanosheets, 20 mM EDTA, and 2 μM 22-C.

clearly indicated that with the increase of ssDNA adsorbed on β-Ni(OH)$_2$ nanosheets, the quenching efficiency improves. The value of 5-F with 5 bases is about 38%, and the signal-to-noise (S/N) is about 0.6. However, the value of 22-F with 22 bases is about 97%, and the S/N is about 35. This result indicated that the affinity between short ssDNA and β-Ni(OH)$_2$ nanosheets was much weaker than that between ssDNA with long length and nanosheets. In other word, β-Ni(OH)$_2$ nanosheets display different affinity toward short ssDNA with different lengths.

The effect of $MgCl_2$ concentration, β-Ni(OH)$_2$ nanosheets dosages and pH on DNA adsorption is presented in Fig. S1 and S2 Since the quenching efficiency is directly proportional to the amount of DNA adsorbed, we used the quenching efficiency to evaluate the adsorption behavior. As shown in Fig. S1, the adsorption efficiency enhanced with increasing salt concentrantion until the volume of β-Ni(OH)$_2$ nanosheets reached 6 μL, in which β-Ni(OH)$_2$ nanosheets were enough to capture DNA. The higher salt concentration, the less volume of β-Ni(OH)$_2$ nanosheets was used for achieving 100% quenching efficiency. Therefore, DNA adsorption can be conveniently controlled by regulating divalent Mg^{2+} ions.

Since FAM is a pH-sensitive dye, an indirect method was conducted to study the pH effect. Herein, 22-base DNA was mixed with β-Ni(OH)$_2$ nanosheets in five buffers for binding. After absorption, these samples were centrifuged, and the supernatant solution was diluted in a pH 8.0 buffer for quenching efficiency measurement. As the pH reduced from 8.0 to 4.0, the quenching efficiency increased from 45% to 99% (Fig. S2), suggesting the nanosheets were stable unless an incubation in pH 4.0 buffer for 24 h (Fig. S3). The result indicated that absorption was more effective at relatively lower pH.

DNA desorption

Usually, desorption of the adsorbed ssDNA was conducted by adding its complementary DNA to displace and form a duplex.[25,26] Recently, the degradation of nanomaterial has also been proved to be an effective way for DNA desorption. However, such kinds of nanomaterials are rare.[17,30] It is interesting that β-Ni(OH)$_2$ nanosheets can be degraded by heat treating at 95 °C for 5~10 min in the present of EDTA (Fig. S4A), while, they can remain stable when treating with EDTA or heating at 95 °C alone. The reason may be that β-Ni(OH)$_2$ nanosheet is converted to EDTA-Ni^{2+} due to the stronger combining ability between and EDTA Ni^{2+}: [31]

$$Ni(OH)_2 + EDTA \rightarrow EDTA\text{-}Ni^{2+} + 2OH^-$$

However, the reaction rate is very slow at room temperature. Heating can increase the molecular activity, and then the reaction is intensified and completed in a few minutes. Based on this founding, we further test the efficiency of DNA desorption. Before desorption experiment, Cy3 labeled-ssDNA (22-C) was fully absorbed on β-Ni(OH)$_2$ nanosheets to form 22-C/β-Ni(OH)$_2$ nanosheets complex. After desorption, the solution was then centrifuged, and the supernatant was collected for analysis. As shown in Fig. 3, a red precipitation and a low fluorescence signal can be observed when 22-C was absorbed on β-Ni(OH)$_2$ nanosheets (sample b). When treating with EDTA and heating at 95 °C (sample e), the precipitation disappeared and the fluorescence of supernatant enhanced significantly. We defined the fluorescence intensity of the sample containing only 22-C as 100%. Treating with EDTA and heating at 95 °C resulted in ~90% DNA probe desorption, regardless of the pH change (Fig. S5). Additionally, the desorbed DNA probe can also hybridize with complementary DNA to form duplex (Fig. S4B). These results indicate that DNA desorption from β-Ni(OH)$_2$ nanosheet can be effectively induced by degrading the nanosheet, and the desorbed DNA probe also remains active. We further used a molecular beacon (MB) to recognize the desorbed DNA probe (Fig. S6), and found that this specific ability of nanosheet displayed potential application in DNA enrichment.

Feasibility of the β-Ni(OH)$_2$ DSNSA biosensor

β-Ni(OH)$_2$ nanosheets not only display differential affinity toward ssDNA fragment with differential length, but also can efficiently quench fluorescence from the adsorbed DNA probe. In view of the above findings, we used β-Ni(OH)$_2$ nanosheets as a sensor platform and developed a novel β-Ni(OH)$_2$ nanosheets mediated DSNSA (β-Ni(OH)$_2$ DSNSA) assay for the quantification of miRNAs. As shown in Scheme 2, ssDNA with two fluorophores attached at both ends is used as recognition

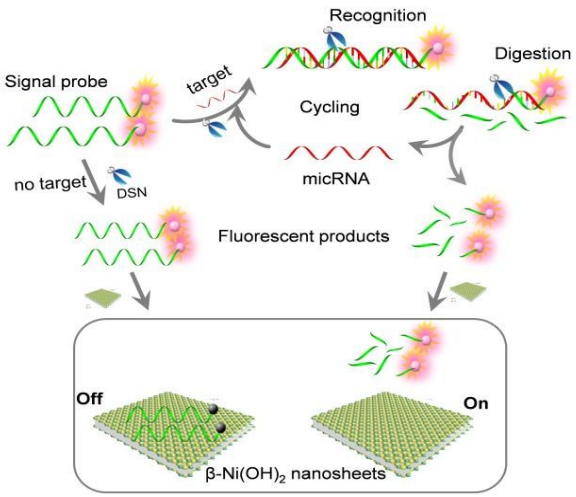

Scheme 2. Schematic illustration of β-Ni(OH)$_2$ DSNSA sensor for miRNA detection.

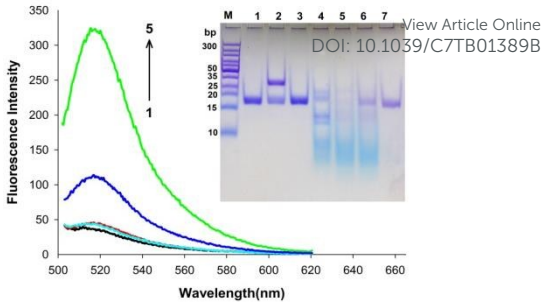

Fig. 4 Fluorescence emission spectra of P-141 and miRNA-141 with DSN. The concentrations of P-141, miRNA-141, DNA-141 and β-Ni(OH)$_2$ nanosheets were 300 nM, 10 nM, 10 nM and 6 μL (480 μg/mL), respectively. Inset: non-denatured PAGE analysis of P-141 and miRNA-141 with DSN. Lane 1: P-141; lane 2: P-141 + miRNA-141; lane 3: P-141 + DSN; lane 4: P-141 + DNA-141 + DSN; lane 5: P-141 + miRNA-141 +DSN; lane 6: P-141 + 2000 nM miRNA-141 + DSN; lane 7: miRNA-141. The concentrations of P-141, miRNA-141 and DNA-141 were 2000 nM, 1000 nM and 1000 nM, respectivel.

probe. The ssDNA can hybridize with the target miRNA and form ssDNA/miRNA duplex, which is perfect substrate for DSN. The DSN then cleaves the ssDNA strand only and releases the target miRNA to further hybridize with another ssDNA, leading to a cyclic DSNSA reaction. The cyclic cleavage of ssDNA will produce numerous short fluorophore-linked oligonucleotide fragments, which are difficult to adsorb on the β-Ni(OH)$_2$ nanosheets due to their weak affinity. Therefore, strong fluorescence signal was obtained. On the contrary, without target miRNA, the ssDNA remains intact and can be captured by β-Ni(OH)$_2$ nanosheets and detected with weak fluorescence.

To demonstrate the feasibility of the β-Ni(OH)$_2$ DSNSA assay for miRNA detection, miRNA-141 was selected as model target. FAM-labeled ssDNA (P-141) which is complementary to miRNA-141 was prepared as recognition probe. Electrophoresis and fluorescent analysis were performed to verify the DSNSA process and β-Ni(OH)$_2$ nanosheets quenching mechanism. As shown in Fig. 4, in the absence of miRNA-141 or DSN, both lane 1 and lane 3 have the same P-141 band, indicating that the P-141 could not be cleaved by DSN in the absence of miRNA-141. After incubating them with β-Ni(OH)$_2$ nanosheets, their fluorescence was almost entirely quenched (curves 1, 3). This could be ascribed to the strong affinity and high fluorescence quenching efficiency of the β-Ni(OH)$_2$ nanosheets for long P-141 probe. However, when half-dosage miRNA-141 was added and incubated with DSN (lane 5), both of P-141 band and new P-141/miRNA-141 hybridize band in lane 2 were disappeared, which were replaced by many short fragments bands. Intact miRNA-141s were also observed in the DSNSA system when we further increased the dosage of miRNA-14 in lane 6. This result indicated that one miRNA-141 can initiate the cyclic cleavage of P-141 and generate numerous short fragments. Strong fluorescence signal was observed (curves 5) due to weak affinity between the short fragments and β-Ni(OH)$_2$ nanosheets. In order to confirm the amplification, a target ssDNA, DNA-141 with same sequences as miRNA-141 (sequence was shown in table S1), was used as a control. In this case, one target can just trigger one cleavage of P-141 because of the complete cleavage of DSN for DNA-DNA duplex. Therefore, there was no signal amplification. Overdose of P-141 band was appeared in lane 4, and lower fluorescence response was present in curve 4. Both of them were different from miRNA-141which can initiate signal amplification (lane 5, curve 5). Those results clearly show that the present method for miRNA determination is feasible.

Detection performance of the β-Ni(OH)$_2$ DSNSA biosensor

The working temperature was further optimized for higher assay performance and it was found that reaction gave the best result at 60 °C (Fig. S7). At this temperature, the P-141/miRNA-141 kept in duplex due to their higher melting temperature (shown in Fig. S8). Under the selected conditions, the response of β-Ni(OH)$_2$ DSNSA assay to various concentrations of miRNA-141 was studied. As shown in Fig. 5A, the fluorescence signal increases dramatically with the increasement of the concentration of miRNA-141 from 0 to 100 nM. A linear relationship is observed with miRNA-141 concentrations in the ranges from 1 pM to 5 nM (R^2 = 0.9962), and the correlation equation is lg (F/F_0) = 0.5702 + 0.1778 lgC, where F and F_0 are the fluorescence intensities at 518 nm in the presence and absence of miRNA-141, respectively. Additionally, fluorescence enhancement can also be found when the target concentration was as low as 1 pM, which is comparable to some previously reported fluorescence sensors. [2,14,32] The excellent sensitivity should be attributed to the strong cleavage activity of DSN and the high fluorescence quenching capability of β-Ni(OH)$_2$ nanosheets. We further test the specificity of proposed miRNA assay by using similar RNA strands with the same concentration (10 nM). As shown in Fig. 5B, the fluorescence response of target miRNA-141 is much higher than that of the similar RNA, including the SmiRNA-141 with single-base-variation from miRNA-141. A consistent result was also achieved with gel study (Fig. S9). These results demonstrate that the approach shows high selectivity toward the target miRNA, which is mainly attributed to the high specificity of DSN enzyme.[2,7,33]

View Article Online
DOI: 10.1039/C7TB01780B

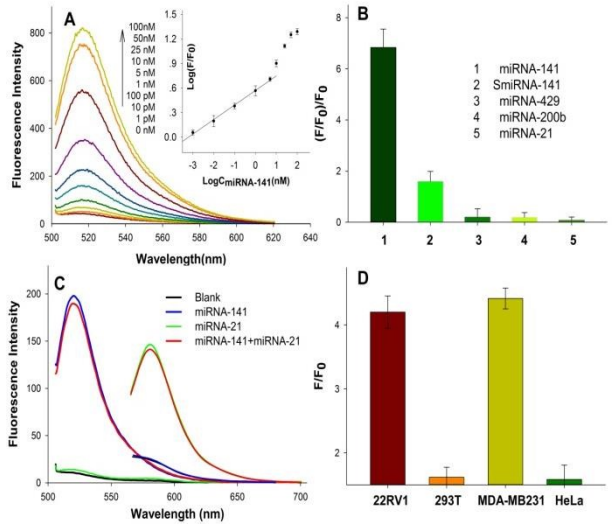

Fig. 5 A) Fluorescence responses of β-Ni(OH)$_2$ DSNSA assay for different concentrations of miRNA-141. Inset is the linear relationship. **B)** Specificity of β-Ni(OH)$_2$ DSNSA assay. Bars represent the fluorescence intensity ratio $(F-F_0)/F_0$ upon the different miRNAs with the same concentration of 10 nM. **C)** Fluorescence responses of β-Ni(OH)$_2$ DSNSA assay for multiplexed detection of miRNA-141 (blue), miRNA-21 (green) or both miRNA-141 and miRNA-21 (red). The concentrations of miRNA were 10 nM. **D)** Fluorescence response of β-Ni(OH)$_2$ DSNSA assay for miRNA-141s in the same dosage of total RNAs isolated from four kinds of human cell lines. Error bars are standard deviation of more than three repetitive experiments.

It is well known that some diseases are related with the abnormal expressions on several miRNAs, the capability of simultaneous analysis for multiple miRNAs is crucial in clinical diagnostics.[34,35] In this respect, we choose miRNA-141 and miRNA-21 as model targets and test multiplex capability of our sensor. As shown in Fig. 5C, two signal probes, P-141 and P-21, labeled with FAM and TAMRA, were perfectly matched with miR-141 and miR-21, respectively. Both of them were prepared in the same sample. In the absence of target miRNAs, the two probes were absorbed and quenched by β-Ni(OH)$_2$ nanosheets. The fluorescence peaks for miRNA-141 and miRNA-21 (518 nm and 580 nm) were very low. When only miRNA-141 or miRNA-21 was present, the sensor only emitted the corresponding fluorescence signal at 518 nm or 580 nm. When all the targets were present, the corresponding fluorescence emissions were observed at both 518 nm and 580 nm. More importantly, the signal response to specific miRNA cannot be influenced by other miRNAs. These results indicate that our sensor is suitable for multiplexed miRNAs detection.

Applicability of the β-Ni(OH)$_2$ DSNSA biosensor

To investigate whether the present method could be applied in real complex biological samples, the expression of miRNA-141 was measured in total RNAs from different cell extracts including the human prostate cancer cell line (22Rv1), cervical cancer cell lines (HeLa), breast cancer cell lines (MDA-MB231) and human embryonic kidney cell line (293T). The total RNAs from human cancer cell lines were divided into two equal parts and detected with the β-Ni(OH)$_2$ DSNSA assay and qRT-PCR, respectively. As shown in Fig. 5D, the results clearly indicated that 22Rv1 and MDA-MB231 cell lines showed higher miRNA-141 expression level in contrast with HeLa and 293T cell lines, which is in good accordance with the results of qPT-PCR (Table S2 in the Supporting Information) and previous reports.[7,36,37] Therefore, this β-Ni(OH)$_2$ DSNSA biosensor could be an effective and reliable method for practical applications towards miRNA detection.

Experimental

Materials and reagents

All oligonucleotides were obtained from Takara Biotechnology Co. Ltd. (Dalian, China). Their sequences were shown in Table S1. Duplex-specific nuclease (DSN) and 10×DSN master buffer (500 mM Tris-HCl, pH = 8.0, 50 mM $MgCl_2$ and 10 mM DTT) were purchased from Newborn Co. Ltd. (Shenzhen, China). Total RNA Extractor, Diethy pyrocarbonate (DEPC) and Low Range DNA Ladder (Thermo scientific, USA) were purchased from Sangon Biotechnology Co. Ltd. (Shanghai, China). Tris and other reagents were obtained from Sinophrm Chemical Reagent Co., Ltd (Shanghai, China). The sterilized water (resistance $\geqslant$18.2 MΩ/cm), tips and tubes were treated with 0.1% DEPC and used throughout the experiments.

Preparation of β-Ni(OH)$_2$ nanosheets

The β-Ni(OH)$_2$ nanosheets were prepared by mixing 50 mL $NiCl_2 \bullet 6H_2O$ aqueous solution (0.05 M) with 50 mL NH_3 aqueous solution (0.075 M) under vigorous stirring at 60 °C for 24 hours.[38] The mixture was later centrifuged to collect the precipitate. It was rinsed by ethanol and later dried. The final product was dispersed with 10 mL DEPC treated water (about 4.8 mg/mL).

Adsorption efficiency

The adsorption efficiency experiment was carried out by adding 5 μL β-Ni(OH)$_2$ nanosheets solution (480 μg/mL) to 120 μL of DNA solution. After 10 min room temperature incubation for binding, the sample was measured by exciting at 490 nm. The DNA solution was prepared using Tris-HCl buffer (25 mM, pH 8.0, 100 mM KCl, 1 mM $MgCl_2$).

To investigate the effect of pH on adsorption efficiency, several kinds of buffer solutions (25 mM) containing 100 mM KCl were prepared: Tris-HCl (pH 8.0), HEPES (pH 7.0), MES (pH 6.0) and acetate buffer (pH 4.0 and 5.0). Each sample (40 μL) containing β-Ni(OH)$_2$ nanosheets (84 μg/mL) and the 22-mer DNA (22-F) (600 nM) was incubated at room temperature about 45 min for binding. After centrifuging at 10,000 rpm for 10 min, 20 μL of the supernatant solution was transferred into 100 μL of buffer (250 mM Tris HCl, 100 mM KCl, 1 mM $MgCl_2$, pH 8.0). Finally, the samples were measured by exciting at 490 nm. The signal of another sample containing the same ssDNA concentration but without β-Ni(OH)$_2$ nanosheets was defined as 100%.

Desorption of ssDNA

The ssDNA/β-Ni(OH)$_2$ nanosheets complex (25 μL) was prepared by mixing 2.5 μL of Cy3 labeled-ssDNA (22-C, 20 μM)

and 5 μL of β-Ni(OH)$_2$ nanosheets (4.8 mg/mL) in different buffers for 20 min. Desorption experiment was carried out by adding 5 μL EDTA (100 mM) and treating at 95 °C for 10 min. After desorption, the solutions were centrifuged at 10,000 rpm for 2 min. Photographs of these solutions were collected via a Canon digital camera. To test the desorption efficiency, the supernatant solutions were analyzed by electrophoresis and fluorometry. For electrophoresis, 10 μL of the supernatant solution was mixed with the same dosage of DNA-141 to form dsDNA. For fluorometry, the supernatant solution was diluted with 100 μL buffer (different pH), and the samples were measured by exciting at 550 nm.

miRNAs detection

For miRNA detection, the reaction sample (20 μL) was prepared by mixing 300 nM P-141, 0.2 U DSN and different concentrations of target miRNAs in 1×DSN master buffer (50 mM Tris-HCl, pH = 8.0, 5 mM $MgCl_2$ and 1 mM DTT) and incubating at 60 °C for 40 min. The amplified detection of miRNA was performed in a 20 μL reaction mixture containing different concentrations of target miRNAs, 300 nM P-141, 0.2 U DSN and 1×DSN master buffer (50 mM Tris-HCl, pH = 8.0, 5 mM $MgCl_2$ and 1 mM DTT) at 60 °C for 40 min. Then, 6 μL β-Ni(OH)$_2$ nanosheets (480 μg/mL) and 100 μL dilution buffer (20 mM Tris, pH = 8.0, 100 mM KCl, 1 mM $MgCl_2$) were injected. The final mixture was incubated at room temperature for 10 min before fluorescence measurement on a LS-55 Fluorescence Spectrometer (Perkin Elmer, USA). Fluorescence measurements were performed by using the following instrument parameters: excitation wavelengths 490 nm, emission wavelengths 518 nm, excitation slit width 5.0 nm, emission slit width 10 nm, range 500 ~ 650 nm. In the multiplexed detection, the excitation wavelengths were set at 490 nm for P-141 and 550 nm for P-21. Unless otherwise indicated, the oligonucleotides concentration mentioned in this work means the value calculated from the 20-μL reaction mixture.

Gel Electrophoresis

For electrophoresis, the sample was prepared by mixing 2000 nM p-141 with 0.4 U DSN or 1000 nM miRNA in 1×DSN master buffer, followed by incubating at 60 °C for 40 min. The concentrations of miRNA in lane 6 and 7 were 2000 nM. Gel electrophoresis analysis was carried out on 20% (w/w) non-denaturing PAGE gels at 1W power for about 1.5 h in 1 × TBE buffer. After electrophoresis, the gel was stained with Stains-All, eluted with DEPC treated water and visualized via a Canon digital camera.

Cell Extractions and miRNA Analysis

The Hela (human cervical cancer cell lines), MDA-MB231 (breast cancer cell lines), 293T (human embryonic kidney cell line) and 22Rv1 (prostate cancer cell line) cells were obtained from the Type Culture Collection of the Chinese Academy of Sciences (Shanghai, China). All of them were cultured in different mediums supplemented with 10% fetal bovine serum (FBS) at 37 °C under a humidified 5% CO_2 atmosphere. The mediums of Hela, MCF-7 and 293T were DMEM. The mediums of 22RV1 and MDA-MB-231 were RPMI-1640 and L-15, respectively. For the preparation of cellular extracts sample, cells (~3×10^7 cells) were washed twice with PBS (137 mM NaCl, 2.7 mM KCl, 10 mM phosphate, pH 7.4). Then, an appropriate amount of Trizol Reagent (Sangon Biotech Co. Ltd., Shanghai, China) was added to ensure full cell disruption. The solution was divided into two equal parts. One was used to extract total RNA according to the manufacturer protocols and analysed with the β-Ni(OH)$_2$ nanosheet DSNSA assay. The other was send to testing company (Sangon Biotech Co. Ltd., Shanghai, China) and analyzed with qRT-PCR.

Conclusions

In summary, we firstly report that β-Ni(OH)$_2$ nanosheets can selectively absorb ssDNA on the surface with a high affinity and subsequently quenched the adsorbed fluorescent-labeled ssDNA with high efficiency. The systematical study of the absorption and desorption behavior of ssDNA on β-Ni(OH)$_2$ nanosheets has shown that the absorption can be modulated by changing the cations, pH and the length of ssDNA, and that the desorption can occur by degrading the β-Ni(OH)$_2$ nanosheets. β-Ni(OH)$_2$ nanosheet was successfully used as a fluorescent sensing platform and a new DSNSA strategy was developed for miRNA detection. Combining the super fluorescence quenching ability of the β-Ni(OH)$_2$ nanosheets and the advantage of DSNSA, this strategy exhibited extraordinary sensitivity, selectivity and multiplex detection capability. As an effective fluorescent sensing platform, β-Ni(OH)$_2$ nanosheets show great potential application in nucleic acid-based optical sensor for clinical diagnostics..

Acknowledgements

We are grateful to the National Natural Science Foundation of China (Grants No. 21405023, 21665010 and 51302117), the outstanding youth fund of Jiangxi Province (20162BCB23027), Natural Science Foundation of Jiangxi Province (Grant No. 20171BAB203015, 20161BAB203097 and 20151BAB203018), and the State Key Laboratory of Chemical Biosensing & Chemometrics (Grant No. 2015010 and 2013012) for their financial support of this work.

References

1 M. I. Almeida, R. M. Reis and G. A. Calin, *Mutat Res, Fundam Mol Mech Mutagen,* 2011, **717**, 1.
2 F. Degliangeli, P. Kshirsagar, V. Brunetti, P. P. Pompa and R. Fiammengo, *J. Am. Chem. Soc,* 2014, **136**, 2264.
3 S. Fleige and M. W. Pfaffl, *Mol. Aspects. Med.* 2006, **27**, 126.
4 C. Becker, A. I. Hammerle-Fickinger and M.W. P. Riedmaier, *Methods*, 2010, **50**, 237.
5 Y.Q. Cheng, X. Zhang, Z. P. Li, X. X. Jiao, Y. C. Wang and Y. L. Zhang, *Angew. Chem. Int. Ed.* 2009, **48**, 3268.
6 J. Van Ness, L. K. Van Ness, and D. J. Galas, *PNAS*. 2003, **100**, 4504.
7 B. C. Yin, Y. Q. Liu and B. C. Ye, *J. Am. Chem. Soc,* 2012, **134**, 5064.

View Article Online
DOI: 10.1039/C7TB01389B

8 Q. Xi, D. M. Zhou, Y. Y. Kan, J. Ge, Z. K. Wu, R. Q. Yu and J. H. Jiang, *Anal. Chem,* 2014, **86**, 1361.
9 S. B. Ni, X. H. Lv, T. Li, X. L. Yang and L. L. Zhang, *J. Mater. Chem. A,* 2013, **1**, 1544.
10 H. X. Li, Y. H. Yu, M. B. Starr, Z. D. Li and X. D. Wang, *J. Phys. Chem. Lett.,* 2015, **6**, 3410.
11 J. Y. Ji, L. L. Zhang, H. X. Ji, Y. Li, X. Zhao, X. Bai, X. B. Fan, F. B. Zhang, and R. S. Ruoff, *ACS Nano,* 2013. **7**, 6237.
12 Y. Q. Miao, L. Ouyang, S. L. Zhou, L. Xu, Z. Y. Yang, M. S. Xiao, and R. Z. Ouyang, *Biosens. Bioelectron.* 2014, **53**, 428.
13 J. Ge, L. J. Tang, Q. Xi, X. P. Li, R. Q. Yu, J. H. Jiang and X. Chu, *Nanoscale,* 2014, **6**, 6866.
14 T. Y. Wang, R. Z. Zhu, J. Q. Zhuo, Z. W. Zhu, Y. H. Shao, and M. X. Li, *Anal. Chem,* 2014, **86**, 12064.
15 Y. X. Yuan, R. Q. Li and Z. H. Liu, *Anal. Chem,* 2014, **86**, 3610.
16 H. H. Fan, Z. L. Zhao, G. B. Yan, X. B. Zhang, C. Yang, H. M. Meng, Z. Chen, H. Liu and W. H. Tan, *Angew. Chem. Int. Ed,* 2015, **127**, 4883.
17 Z. L. Zhao, H. H. Fan, G. F. Zhou, H. R. Bai, H. Liang, R. W. Wang, X. B. Zhang and W. H. Tan, *J. Am. Chem. Soc.* 2014. **136**, 11220.
18 Y. Cen, Y. Yang, R. Q. Yu, T. T. Chen and X. Chu, *Nanoscale,* 2016, **8**, 8202.
19 C. Lu, Y. B. Liu, Y. B. Ying and J. W. Liu. *Langmuir,* 2017, **33**, 630.
20 P. Alonso-Cristobal, P. Vilela, A. El-Sagheer, E. Lopez-Cabarcos, T. Brown, O. L. Muskens, J. Rubio-Retama and A. G. Kanaras. *ACS Appl. Mater. Interfaces,* 2015, **7**, 12422.
21 P. Vilela, A. El-Sagheer, T. M. Millar, T. Brown, O. L. Muskens and A. G. Kanaras. *ACS Sens.,* 2017, **2**, 52.
22 S. H. Jiang, Z. Gui, G. H. Chen, D. Liang and J. Alam, *ACS Appl Mater,* 2015, **7**, 14603.
23 M. Aghazadeh, A. N. Golikand and M. Ghaemi, *Int J Hydrogen Energy,* 2011, **36**, 8674.
24 S. Cabanas-Polo, B. Ferrari and A. J. Sánchez-Herencia, *Boletín de la Sociedad Española de Cerámicay Vidrio,* 2014, 53, 265.
25 B. W. Liu, Z. Y. Sun, X. Zhang, J. and W. Liu, *Anal. Chem,* 2013, **85**, 7987.
26 M. Wu, R. Kempaiah, P. J. Huang, V. Maheshwari and J. W. Liu. *Langmuir*, 2011, **27**, 2731.
27 J. W. Liu and Y. Lu, *J. Am. Chem. Soc.,* 2007, **129**, 9838.
28 D. G. He, X. X. He, K. M. Wang, X. Yang, X. X. Yang, X. C. Li and Z. Zou, *Chem. Commun,* 2014, **50**, 11049.
29 M. Chhowalla, H. S. Shin, G. Eda, L. J. Li, K. P. Loh and H. Zhang, *Nat Chem,* 2013, **5**, 263.
30 R. R. Deng, X. J. Xie, M. Vendrell, Y. T. Chang, and X. G. Liu, *J. Am. Chem. Soc.* 2011, **133**, 20168.
31 F. L. Fu, B. Tang, Q. Wang, J.Y. Liu, *Environ Chem Lett*, 2010, **8**, 317.
32 X. Y. Lin, C. Zhang, Y. S. Huang, Z. Zhu, X. Chen and C. Y. Yang, *Chem. Commun*, 2013, **49**, 7243.
33 X. P. Qiu, H. Zhang, H. L. Yu, T. L. Jiang and Y. Luo, *Trends Biotechnol*, 2015, **33**, 180.
34 J. Lu, G. Getz, E. A. Miska, E. Alvarez-Saavedra, J. Lamb, D. Peck, A. Sweet-Cordero, B. L. Ebert, R. H. Mak, A. A. Ferrando, J. R. Downing, T. Jacks, H. R. Horvitz and T. R. Golub, Nature, 2005, **435**, 834.
35 C. Y. Yang, B. T. Dou, K. Shi, Y. Q. Chai, Y. Xiang and R. Yuan, *Anal. Chem,* 2014, **86**, 11913.
36 K. P. Porkka, M. J. Pfeiffer, K. K. Waltering, R. L. Vessella, T. L. J. Tammela, T. Visakorpi, *Cancer Res*, 2007, **67**, 6130.
37 Q. Wang, Q. Li, X. H. Yang, K. M. Wang, S. S. Du, H. Zhang and Y. J. Nie, *Biosens. Bioelectron,* 2016, **77**, 1001.
38 L. B. Li, C. Wang, K. Y. Liu, Y. H. Wang, K. Liu and Y. Q. Lin, *Anal. Chem.,* 2015, **87**, 3404.

View Article Online
DOI: 10.1039/C7TB01389B

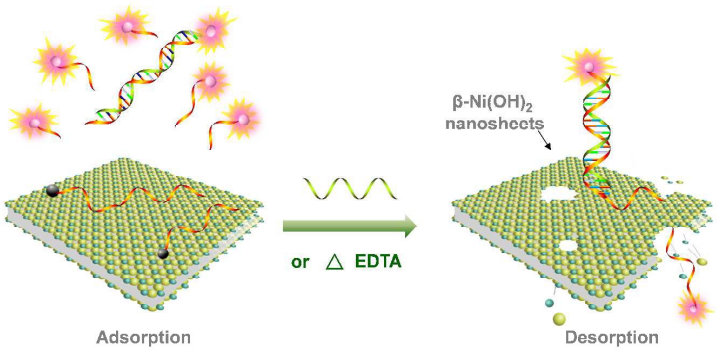

TOC

We report for the first time that β-$Ni(OH)_2$ nanosheet can exhibit differential affinity toward short oligonucleotide fragment versus ssDNA probe and the absorbed DNA can also been desorbed by degrading the β-$Ni(OH)_2$ nanosheet.